Key Points:
- A hyperbola-shaped feature is observed in the MARSIS echograms over an isolated region of strong crustal magnetic fields on dayside
- A plasma cavity in the upper ionosphere and a density enhancement in the lower ionosphere are observed too
- Energization by downward acceleration of solar wind electrons and upward acceleration of ionospheric ions may explain the plasma loss

A case study of a density structure over a vertical magnetic field region in the Martian ionosphere

F. Duru[1,2], D. A. Gurnett[1], C. Diéval[5], D. D. Morgan[1], D. Pisa[1,3], and R. Lundin[4]

[1]Department of Physics and Astronomy, University of Iowa, Iowa City, Iowa, USA, [2]Department of Physics, Coe College, Cedar Rapids, Iowa, USA, [3]Institute of Atmospheric Physics CAS, Prague, Czech Republic, [4]Swedish Institute of Space Physics, Umeå, Sweden, [5]Lancaster University, Lancaster, UK

Abstract One of the discoveries made by the radar sounder on the Mars Express spacecraft is the existence of magnetically controlled structures in the ionosphere of Mars, which result in bulges in the ionospheric electron density contours. These bulges lead in turn to oblique echoes, which show up as hyperbola-shaped features in the echograms. A hyperbola-shaped feature observed over an isolated region of strong crustal magnetic field is associated with a plasma cavity in the upper ionosphere and a corresponding density enhancement in the lower levels of the ionosphere. We suggest that along open magnetic field lines, the solar wind electrons are accelerated downward and the ionospheric ions are accelerated upward in a manner similar to the field line-driven auroral acceleration at Earth. This heating due to precipitating electrons may cause an increase in the scale height and may drive a loss of ionospheric plasma at high altitudes.

1. Introduction

The Mars Advanced Radar for Subsurface and Ionospheric Sounding (MARSIS) [*Picardi et al.*, 2004], which is one of the six instruments on board Mars Express spacecraft, in orbit around Mars since 2003, has provided many interesting findings about the Martian ionosphere. One of these findings is the existence of magnetically controlled structures in the ionosphere of Mars [*Gurnett et al.*, 2005; *Duru et al.*, 2006; *Gurnett et al.*, 2008; *Andrews et al.*, 2014; *Diéval et al.*, 2015]. These authors showed that these magnetically controlled features are seen as hyperbola-shaped traces in the MARSIS echograms, which are displays of echo intensity as a function of apparent altitude and time. The first panel of Figure 1 is an example of an echogram. These previous studies show that the hyperbola shaped features are oblique reflections from regions of enhanced electron density that are fixed with respect to Mars, while a vertical echo is reflected from the horizontally stratified ionosphere, which is seen as an almost horizontal line at around 130 km altitude in the figure. Comparisons with the model of *Cain et al.* [2003] for the crustal magnetic field of Mars, hereafter "the Cain model," show that the apexes of the hyperbolas, which identify the closest approach to the regions of enhanced electron density, usually coincide with regions where the crustal magnetic field is significant and nearly vertical and are repetitively observed during passes over these areas [*Gurnett et al.*, 2005; *Duru et al.*, 2006; *Gurnett et al.*, 2008; *Andrews et al.*, 2014; *Diéval et al.*, 2015].

In this paper, we present a case in a particular region on Mars, where the crustal magnetic field is strong with a quickly varying orientation. We have looked at several passes that go through a region around the equator at west longitudes between 295° and 310°. It is a region where the crustal magnetic field shown by the Cain model is strong and nearly vertical (reaching up to 400 nT at 150 km altitude). The MARSIS passes we studied have near-longitudinal trajectories, crossing the region where a strong and almost vertical magnetic field occurs above a limited region. At all times except that short period of time, the magnetic field is featureless and weak. One striking observation is that in each pass, the location where the crustal field is strong and vertical corresponds to the apex of a hyperbola shaped feature in the echogram. In this paper, we examine one such pass along the orbit 11547, from 28 January 2013.

This pass is studied by using data from two instruments on Mars Express: MARSIS and the Analyzer of Space Plasmas and Energetic Atoms (ASPERA-3) [*Barabash et al.*, 2006]. MARSIS is a low-frequency radar sounder, which provides local electron densities and magnetic fields, in addition to the remote sounding of the ionosphere. In the remote sounding mode, a quasi-sinusoidal pulse is transmitted in every direction, and the time delay of the returning echo is recorded. The echo is obtained only when there is a normal incidence

Orbit 11547   January 28, 2013
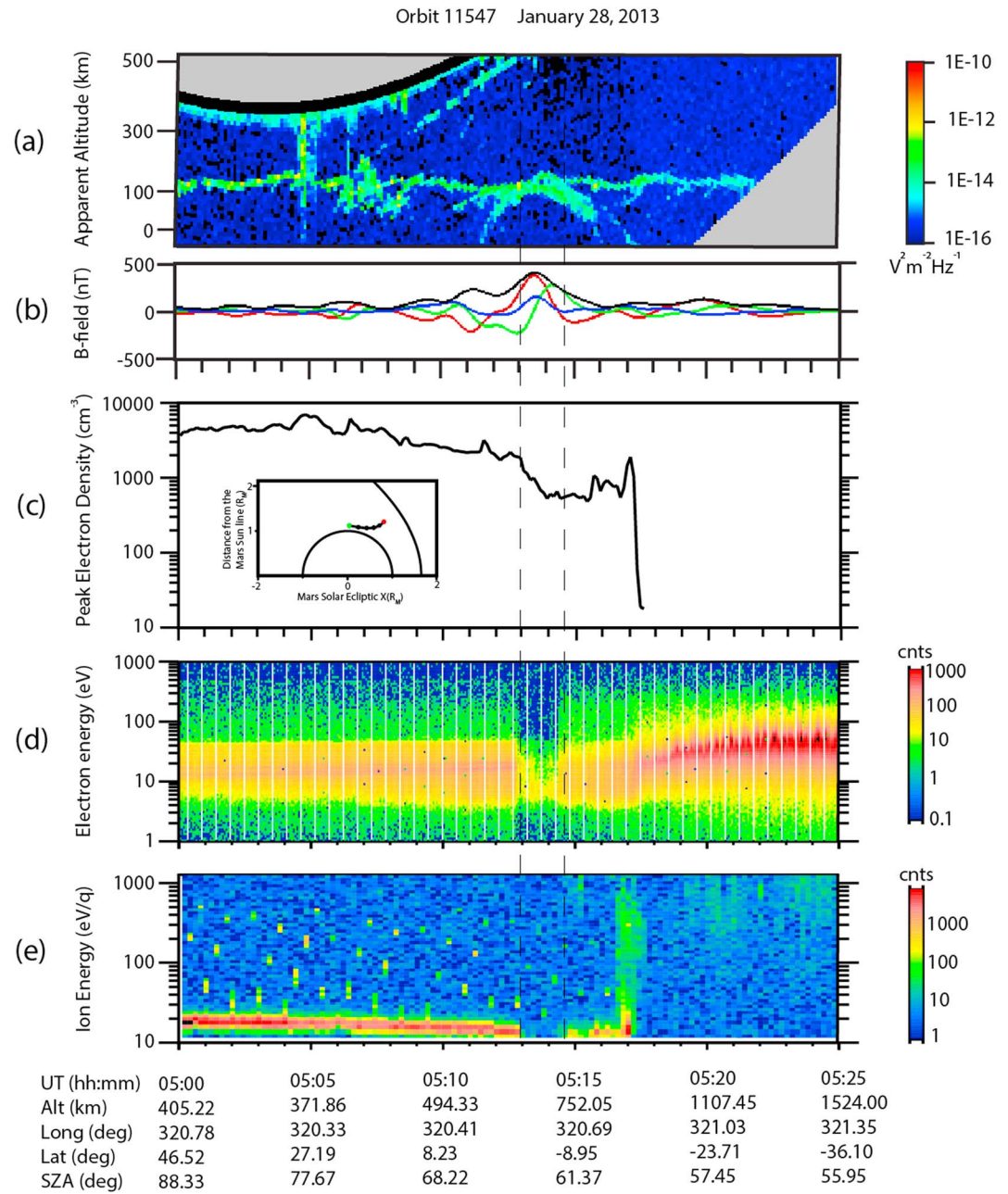
Figure 1. The pass on 28 January 2013. The UT, altitude, longitude, latitude, and SZA values are provided at the bottom of the figure. (a) Echogram from MARSIS. The color bar provides the intensity of the echo. (b) The magnetic field from *Cain et al.* [2003] model at an altitude of 150 km, where red, blue, green, and black lines are vertical, southward, eastward components, and magnitude of the magnetic field, respectively. (c) Local electron density data from MARSIS. A sketch of the trajectory is also provided. (d) Local electron energy-time spectrogram from ELS. (e) Local ion energy-time spectrogram from IMA.

to the ionosphere, where the frequency of the pulse is equal to the electron plasma frequency, f_p. The remote sounding provides the electron density values in the altitude range between 130 and 400 km. With MARSIS, the electron densities at the location of the spacecraft are obtained thanks to the excitation of electron plasma oscillations at the local electron plasma frequency. In many cases, the harmonics of the basic plasma oscillations are used to obtain the local electron plasma frequency. For more information on acquisition of the local electron density, see *Duru et al.* [2008] and *Morgan et al.* [2013].

ASPERA-3 is designed to study the energetic neutral atom and plasma environment of Mars. In this paper, data from the electron spectrometer (ELS) and the ion mass analyzer (IMA) are used to further investigate the case in question. ELS is an electron sensor and has a field of view of $360° \times 4°$ [*Barabash et al.*, 2006; *Frahm et al.*, 2006]. In the mode used here ELS measures electron distributions from 5 eV to 20 keV at a 4 s time resolution. IMA is an ion sensor, made of an electrostatic deflector, which provides the field of view up to $360° \times \pm 45°$ in 16 steps of elevation ($360° \times 4.5°$ per 12 s elevation step), an electrostatic top hat analyzer, which measures ion distributions from ~10 eV/q to 20 keV/q, and a magnetic filter allowing a mass per charge spectrum up to about 80 amu/q [*Barabash et al.*, 2006]. In the mode used here, IMA sweeps through 16 elevation angles in 192 s.

2. Data

The MARSIS orbit we investigate is a 44 min pass, which starts at 04:41 UT, on the nightside at a solar zenith angle (SZA) of 117°, and it proceeds toward the dayside as it approaches the periapsis of altitude ~ 365 km at 05:03 UT. Figure 1 shows the part of this pass that we are interested in, which is at an almost constant western longitude, 320–321°, with a latitude changing from about 45° to −36° and the SZA going from 88 to 56°. The near-longitudinal spacecraft trajectory crosses the equator at about 05:12 UT. Figure 1a shows the MARSIS echogram for this pass, averaged for the frequencies between 1.52 MHz (28.6×10^3 cm^{-3}) and 1.56 MHz (30.2×10^3 cm^{-3}). Figure 1b shows the magnetic field from the Cain model, at an altitude of 150 km. The magnetic field magnitude (black line), and the radial (red line), southward (blue line), and eastward (green line) components of the magnetic field are shown in this panel. Figure 1c displays the local electron density in logarithmic scale obtained from electron plasma oscillations with MARSIS. Finally, Figures 1d and 1e show data from the ASPERA-3 instrument. Figure 1d displays the electron energy time spectrogram in unit of counts from ELS, and Figure 1e presents the ion energy time spectrogram in unit of counts from the IMA, both local to the spacecraft.

In Figure 1a, the almost horizontal line at around 130 km apparent altitude is the echo from the horizontally stratified ionosphere. A hyperbola-shaped echo is observed with the apex at about 5:14 UT. Some half hyperbola features are also seen at around 05:06 UT, 05:09 UT, 05:17 UT, and 05:20 UT. However, even though the apexes of these small features correspond to the places where the radial component of the crustal fields is higher than the southward and eastward components (as shown on Figure 1b), both the magnetic field and hyperbola features are small in these cases, so this paper focuses on the much larger hyperbolic trace with apex time at around 05:14 UT. The spacecraft goes through a particular region where the crustal magnetic field is weak and featureless except around the equator, where it becomes strong and almost vertical. The location of almost vertical, strong magnetic field corresponds to the hyperbola-shaped feature with apex at 05:13:50 UT in the MARSIS echogram given in Figure 1a.

In the figure, the spacecraft starts from an altitude of about 405 km. The corresponding local electron densities are around 4500 cm^{-3}. As the spacecraft starts the ascent in its trajectory after the periapsis, the local electron density decreases slowly. However, when the spacecraft reaches the location of the strong, vertical magnetic field, the local density shows a much stronger and more sudden decrease, dropping by 70% from a background value of 2000 cm^{-3} down to a dip at 600 cm^{-3}. This decrease lasts 1.5 more minutes after the apex of the hyperbola, and then it is followed by an increase in the density at the end of the region in question. After about 05:17 UT, the local electron density values are not obtained since the electron plasma oscillations are not detected anymore. This is due to the fact that the spacecraft crosses the so-called "flow velocity boundary," after which it is in the magnetosheath where the plasma is hot, fast flowing, and less dense [*Duru et al.*, 2010].

Mars Express is in the ionosphere between 05:00 UT and 05:17 UT, as evident from the low-energy ionospheric heavy ions and from the photoelectron peaks generated by photoionization of CO_2 [e.g., *Frahm et al.*, 2006]. A spacecraft charging of about −10 V (normal for the dayside ionosphere) is evident from the shifting of the photoelectron peaks from their nominal energy 21–24 and 27 eV down to 10–20 eV. This negative potential causes the low-energy ions to be detectable above the IMA energy threshold of 10 eV/q. One can also see an artifact caused by the operation of MARSIS in the IMA data: numerous dot-like spikes of ion flux between 30 and 500 eV. After 05:17 UT, Mars Express enters the magnetosheath, recognized by solar wind ions of keV energy and by high fluxes of electrons between 10 and 200 eV.
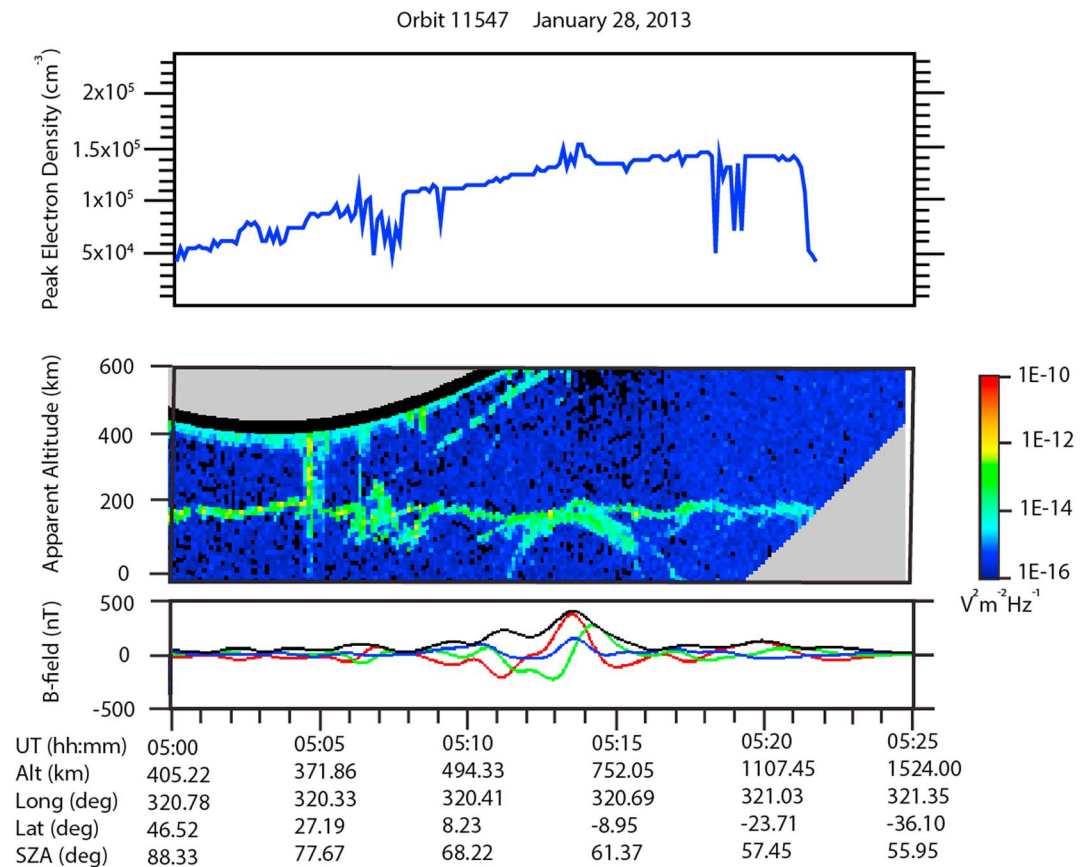
Figure 2. (middle and bottom) Same as in Figure 1. (top) The peak electron density data obtained by remote sounding by MARSIS.

Between 05:13 UT and 05:14:30 UT, both the electron and ion fluxes show a large depletion, which is consistent with the localized drop in the local electron density data from MARSIS. There are also signatures of accelerated O^+ and O_2^+ flowing upward and tailward close to the cavity, with 1–2 keV energy at 05:14:30–05:15 UT and a continuous acceleration all the way from 10 eV to 1 keV at 05:16:30–05:17:30 UT. However, there is no evidence of ongoing plasma acceleration in the cavity itself.

In Figure 2, the top displays the peak electron density in the ionosphere obtained with MARSIS remote sounding. Figures 2 (middle) and 2 (bottom) show the crustal fields from the Cain model and the MARSIS echogram. According to Figure 2 (top), the peak electron density increases gradually, with decreasing SZA as the spacecraft approaches the region of the hyperbola in question, located at SZA = 60°. It shows a localized increase, rising by 23% to 1.6×10^5 cm^{-3} from a background of about 1.3×10^5 cm^{-3}, at the location of the apex of the hyperbola. Then the peak density returns to a steady and slow background value increase for about 4 min. Note that there are some other peaks and dips in the peak density.

3. Discussion and Conclusions

The apex of the hyperbola-shaped echo seen with MARSIS remote sounding data at 05:13:50 UT is at the location where the crustal magnetic field is almost vertical. Also, a depletion is observed at the same time in the local electron flux and the ion flux from ASPERA-3 and in the local electron density data from MARSIS. However, the peak electron density from remote sounding shows an abrupt rise coincident with the observations.

Even though we do not see direct evidence of plasma acceleration at the location of the hyperbola in our data, we propose that at one point in time electrons were accelerated downward and ions were accelerated

upward along open magnetic field lines in a manner similar to the field line-driven auroral acceleration on Earth [*Mauk and Bagenal*, 2013]. The cavity region may be a low-density ionospheric region subjected to plasma acceleration and outflow. We suggest that on the near-vertical crustal field lines, open to the access of solar wind plasma through magnetic reconnection with the interplanetary magnetic field, parallel electric fields may lead to the acceleration of electrons and ions. Precipitating electrons with energies > 300 eV, a typical energy at which auroral electrons are observed on Mars [see, e.g., *Lundin et al.*, 2006], can penetrate down to an altitude of 140 km [*Detrick et al.*, 1997], which is a typical altitude for the main ionospheric peak at SZA $= 60°$ [*Morgan et al.*, 2008]. An increase in the scale height is observed in locations where crustal magnetic fields are almost vertical [e.g., *Ness et al.*, 2000]. The solar wind electrons which penetrate to the lower levels of the ionosphere along vertical magnetic field lines may cause heating and ionization of the atmospheric neutrals and an increase in the scale height [*Gurnett et al.*, 2005; *Ness et al.*, 2000]. *Krymskii et al.* [2002] claim that the increase is due to the heating of the neutral atmosphere by electron impact. The fact that the altitude of the apex of the hyperbola shaped echo is greater than the surrounding ionosphere supports the existence of an upward bulge (higher electron density at a given altitude relative to the surrounding ionosphere), as it is seen by the MARSIS remote sounding data. Energization of the ionospheric plasma by energy input from precipitating solar wind plasma may have caused an outflow of ionospheric plasma to interplanetary space [*Lundin et al.*, 2004] and therefore leaving holes at high altitudes, as ELS, IMA, and MARSIS local density data suggest. An outflow of ionospheric plasma through open field lines is observed also on Earth. Part of the process happening in this case could be similar to the so-called polar wind on the Earth [*Banks and Holzer*, 1968]. The polar wind is the constant outflow of plasma to interplanetary space. The Earth's vertical magnetic fields connect to the solar wind causing the plasma to flow outward into interplanetary space from the ionosphere.

The most suitable explanation for the hyperbola shaped echoes on the MARSIS echograms is the presence of ionospheric bulges. These bulges were attributed to the heating from solar wind precipitation at the locations of vertical crustal fields [*Gurnett et al.*, 2005; *Duru et al.*, 2006] or alternatively attributed to heating by ionospheric currents in areas of open field lines in the dynamo region of Mars [*Andrews et al.*, 2014]. In a statistical study of oblique echoes observed by MARSIS, *Diéval et al.* [2015] have tested the role of heating by precipitating solar wind electrons as an explanation for the bulges and discussed other physical processes which may result in bulges. They concluded that the density structures causing the oblique echoes formed recurrently in areas where near-vertical crustal fields are often closed on dayside (i.e., not reconnected with the interplanetary magnetic field). Closed field lines, with both ends anchored to the crust, prevent the access by solar wind electrons to low altitudes. They also concluded that solar wind precipitation is not necessary to the formation of bulges and that other more recurrent physical processes may result in bulges. For example, a recent 2-D model of the dayside Martian ionosphere, including field aligned transport of plasma [*Matta et al.*, 2015], reproduces electron density contours at an elevated altitude in areas of vertical open field lines, compared to areas of field lines closed on the dayside. *Matta et al.* [2015] explained that plasma diffusion along the vertical field lines may be responsible for the observations of bulges in these areas. Nevertheless, solar wind precipitation with sufficient energy to reach the altitudes of a previously formed bulge (perhaps by heating from ionospheric currents or diffusion along vertical field lines) may cause heating and ionization further enhancing this structure.

As mentioned, the fact that the apexes of the hyperbolas were above the altitude of the regular ionospheric echo supported the hypothesis of bulges [*Duru et al.*, 2006]. To illustrate this explanation, a reflection layer with a constant density in the ionosphere was modeled. A simple geometric simulation for the echogram of the pass on 28 January 2013 shown in Figure 1 was computed. At each point of the reflection layer a perpendicular vector representing the reflected waves of the MARSIS sounder was reproduced. Under an assumption of a free space propagation of waves, both dispersion and refraction were neglected. Therefore, waves can be represented as straight rays propagating at the speed of light. Consequently, the intersections of the ray path with the satellite's altitude were found. The apparent altitudes from a length of the received ray at each position were calculated. Results of this simulation are shown in Figure 3. Figure 3 (top) presents a detail of the reflection layer with a constant altitude of 100 km and a superposed Gaussian shaped bulge (height $= 30$ km; width $= 10$ km) centered at latitude of $-3°$. The color represents three individual parts of the reflection layer. The constant layer altitude is shown by the black color, blue color delimits the layer up to the inflection point of the bulge, and red color presents the vicinity of the bulge top.
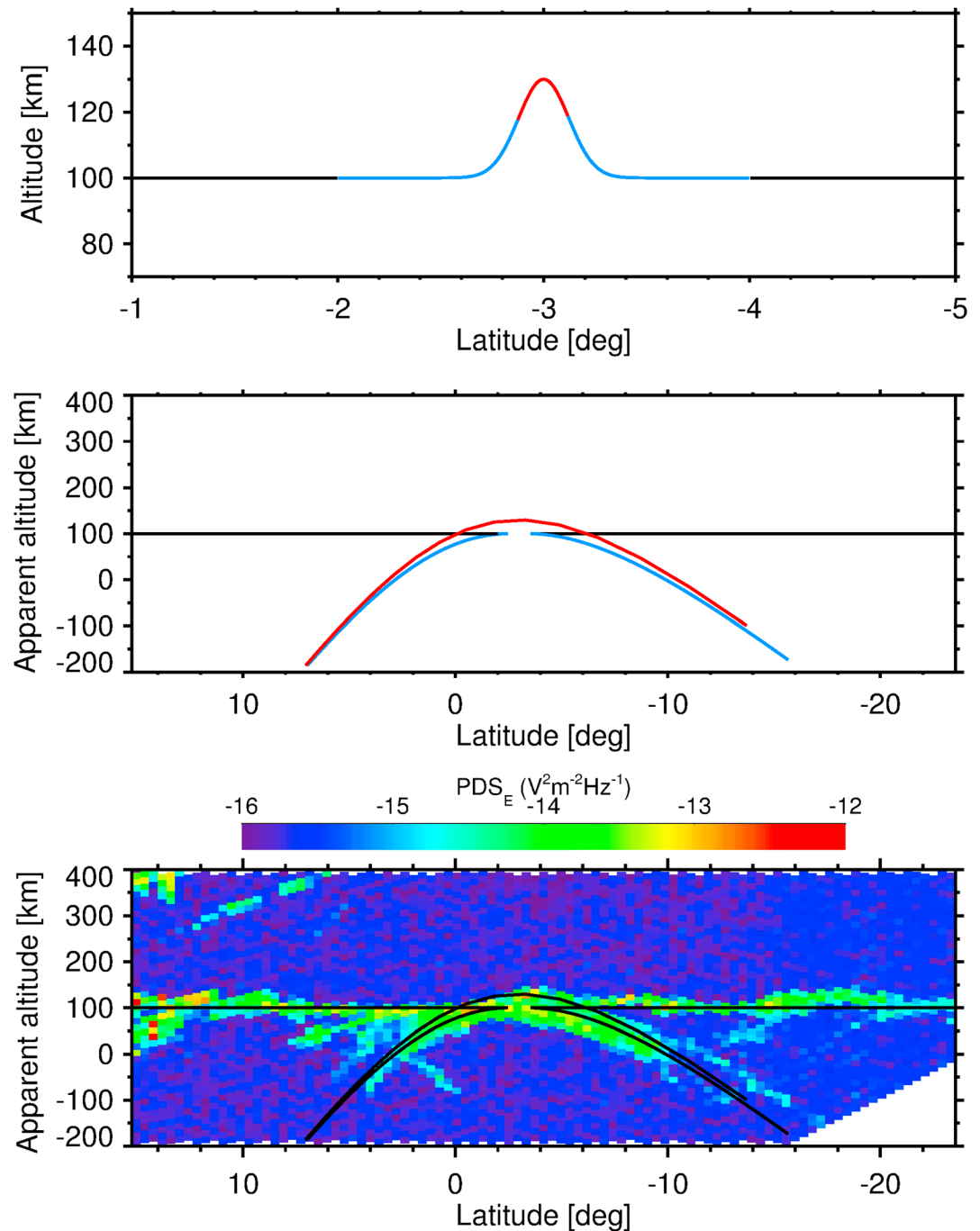
Figure 3. Illustration of the echogram obtained from the modeled ionospheric reflection layer using simple ray propagation. (top) A detail of a reflection layer with the Gaussian shaped bulge (height = 30 km; width = 10 km) superposed on the constant reflection layer with an altitude of 100 km. Three individual parts of the reflection layer are emphasized by colors. (middle) Apparent altitudes calculated from a length of straight rays received at the satellite's altitude are shown. Colors show the reflection from the individual part of the ionospheric layer. (bottom) The echogram presented in Figures 1 and 2. However, it should be noted that the color bar used here is different than the previous two figures. The black line represents the apparent altitude obtained from the simulation.

The apparent altitudes calculated from the ray path simulation are shown in Figure 3 (middle). When the satellite was moving from higher latitudes on the Northern Hemisphere to the equator, the reflection from the constant layer (black color) can be seen. Three points reflection can be observed for latitudes from 7 to -2.8 and -3.2 to $-14°$. The single reflection from the top of the bulge can be seen for latitudes between

−2.8 and −3.2°. The single reflection from the constant layer can be again detected when the satellite was further from the bulge for latitudes lower than −16°. Figure 3 (bottom) shows the observed echogram overplotted by the simulated echogram (the black line). The results of the simple simulation are in almost perfect match with the observations. This is a demonstration that a bulge in the ionosphere would result in a hyperbola-shaped echo on the echograms.

We note that *Nielsen et al.* [2007] also reported cases of localized increases in the peak electron density at the locations of strong near-vertical crustal fields, for which they found no simultaneous observations of energetic particles/radiation, which could have caused the enhancements. Instead, they proposed that the density increases may be caused by a reduction of the ion-electron recombination rates by Joule heating of the neutral atmosphere from AC electric fields associated to plasma instabilities in areas of open magnetic field lines connected to the interplanetary space. It is possible that this phenomenon was occurring here, leading to the observed increased peak density similar to the ones reported by *Nielsen et al.* [2007]. Note that while bulges are frequently observed over near-vertical crustal fields on dayside, the cases of high peak density reported by *Nielsen et al.* [2007] in these areas on dayside were only case studies. Also, a search for increased peak densities at the locations of near-vertical crustal fields over 10 Mars Express orbits gave negative results, indicating that the recurrent bulges may exist independently from the sporadic increased peak densities.

A possible explanation for the observed density depletion (seen in Figures 1c–1e) at high altitudes is the occurrence of a strong wave activity at this location [*Lundin et al.,* 2011]. Although we know that the crustal magnetic field is vertical, we do not have adequate data of the field lines being open to give place to reconnection with the interplanetary magnetic field. The density decrease is due to ions and electrons, moving away from this location, but not necessarily due to escape. The wave activity gives an additional pressure to compensate for the low plasma pressure so that the pressure balance should be maintained across the Mars Express pass above this region. Wave activity may be caused by an (earlier) energy input of solar wind, and it could provide the necessary energy for the particles to move away.

We can rule out motion of the ionosphere-magnetosheath boundary as an explanation for the following reasons: (1) There is no evidence of magnetosheath plasma in the ASPERA-3 data at this location, and (2) the local electron density is not lost during the hyperbola feature.

4. Summary

We have studied a dayside MARSIS pass in a particular region, which displays a strong, vertical magnetic field in a small area, with otherwise very low and featureless magnetic field. A hyperbola-shaped echo is observed on the MARSIS echograms at the location of the strong, vertical magnetic field, indicating the presence of an ionospheric bulge at this location, a feature commonly observed over near-vertical crustal fields on the dayside. Meanwhile, a depletion in the local ion and electron fluxes is observed with the ASPERA-3 instrument, and a drop in the local electron density is seen by MARSIS at the same location. Finally, MARSIS remote sounding data show a small increase in the electron peak density at the location of the near-vertical crustal field, which may be a sporadic feature previously reported in case studies by *Nielsen et al.* [2007], which attributed them to reduced ion-electron recombination rates due to an increased plasma temperature linked to local processes on open magnetic field lines. Our data suggest that a field line-driven auroral acceleration type event occurred, where electrons accelerated downward heating the ionosphere may have provided plasma energization leading to ionospheric outflow, while the loss of plasma at the altitude of the spacecraft may have been caused by upward accelerated ions.

The bulge itself may be first formed from a recurrent mechanism independent from the state open or closed of the near-vertical field lines (perhaps from vertical diffusion along these field lines) and was possibly further enhanced by the sporadic heating and ionization from accelerated downward electrons.

References

Andrews, D. J., M. André, H. J. Opgenoorth, N. J. T. Edberg, C. Diéval, F. Duru, D. A. Gurnett, D. Morgan, and O. Witasse (2014), Oblique reflections in the Mars Express MARSIS data set: Stable density structures in the Martian ionosphere, *J. Geophys. Res. Space Physics*, *119*, 3944–3960, doi:10.1002/2013JA019697.
Banks, P. M., and T. E. Holzer (1968), The polar wind, *J. Geophys. Res.*, *73*, 6846–6854, doi:10.1029/JA073i021p06846.
Barabash, S., et al. (2006), The Analyzer of Space Plasmas and Energetic Atoms (ASPERA-3) for the Mars Express Mission, *Space Sci. Rev.*, *126*, 113–164.

Cain, J. C., B. B. Ferguson, and D. Mozzoni (2003), An *n* = 90 internal potential function of the Martian crustal magnetic field, *J. Geophys. Res.*, *108*(E2), 5008, doi:10.1029/2000JE001487.

Detrick, D. L., T. J. Rosenberg, and C. D. Fry (1997), Analysis of the Martian atmosphere for riometry, *Plan. Space Sci.*, *45*(3), 289–294, doi:10.1016/S0032-0633(96)00134-1.

Diéval, C., D. J. Andrews, D. D. Morgan, D. A. Brain, and D. A. Gurnett (2015), MARSIS remote sounding of localized density structures in the dayside Martian ionosphere: A study of controlling parameters, *J. Geophys. Res. Space Physics*, *120*, 8125–8145, doi:10.1002/2015JA021486.

Duru, F., D. A. Gurnett, T. F. Averkamp, D. L. Kirchner, R. L. Huff, A. M. Persoon, J. J. Plaut, and G. Picardi (2006), Magnetically controlled structures in the ionosphere of Mars, *J. Geophys. Res.*, *111*, A11204, doi:10.1029/2006JA011975.

Duru, F., D. A. Gurnett, D. D. Morgan, R. Modolo, A. Nagy, and D. Najib (2008), Electron densities in the upper ionosphere of Mars from the excitation of electron plasma oscillations. *J. Geophys. Res.*, *113*, A07302, doi:10.1029/2008JA013073.

Duru, F., D. A. Gurnett, J. D. Winningham, R. Frahm, and R. Modolo (2010), A plasma flow velocity boundary at Mars from the disappearance of electron plasma oscillations, *ICARUS*, *206*, 74–82, doi:10.1016/j.icarus.2009.04.12.

Frahm, R. A., et al. (2006), Location of atmospheric photoelectron energy peaks within the Mars environment, *Space Sci. Rev.*, *126*, 389.

Gurnett, D. A., et al. (2005), Radar soundings of the ionosphere of Mars, *Science*, *310*, 1929–1933.

Gurnett, D. A., et al. (2008), An overview of radar soundings of the Martian ionosphere from the Mars Express spacecraft, *J. Adv. Space Res.*, doi:10.1016/j.asr.2007.01.062.

Krymskii, A. M., T. K. Breus, N. F. Ness, M. H. Acuna, J. E. P. Connerney, D. H. Crider, D. L. Mitchell, and S. J. Bauer (2002), Structure of the magnetic field fluxes connected with crustal magnetization and topside ionosphere at Mars, *J. Geophys. Res.*, *107*(A9), 1245, doi:10.1029/2001JA000239.

Lundin, R., et al. (2004), *Science*, *305*(5692), 1933–1936, doi:10.1126/science.1101860.

Lundin, R., et al. (2006), Auroral plasma acceleration above Martian magnetic anomalies, *Space Sci. Rev.*, *126*(1-4), 333–354, doi:10.1007/s11214-006-9086-x.

Lundin, R., S. Barabash, E. Dubinin, D. Winningham, and M. Yamauchi, Low-altitude acceleration of ionospheric ions at Mars (2011), *Geophys. Res. Lett.*, *38*, L047064, doi:10.1029/2011GL047064.

Matta, M., M. Mendillo, P. Withers, and D. D. Morgan (2015), Interpreting Mars ionospheric anomalies over crustal magnetic field regions using a 2-D ionospheric model, *J. Geophys. Res. Space Physics*, *120*, 766–777, doi:10.1002/2014JA020721.

Mauk, B., and F. Bagenal (2013), Comparative auroral physics: Earth and other planets, in *Phenomenology Auroral Phenomenology and Magnetospheric Processes: Earth and Other Planets*, edited by A. Keiling et al., pp. 3–26, AGU, Washington, D. C., doi:10.1029/2011GM001192.

Morgan, D. D., D. A. Gurnett, D. L. Kirchner, J. L. Fox, E. Nielsen, and J. J. Plaut (2008), Variation of the Martian ionospheric electron density from Mars Express radar soundings, *J. Geophys. Res.*, *113*, A09303, doi:10.1029/2008JA013313.

Morgan, D. D., O. Witasse, E. Nielsen, D. A. Gurnett, F. Duru, and D. L. Kirchner (2013), The processing of electron density profiles from the Mars Express MARSIS topside sounder, *Radio Sci.*, *48*, 197–207, doi:10.1002/rds.20023.

Ness, N. F., M. H. Acuna, J. E. P. Connerney, A. J. Kliore, T. K. Breus, A. M. Krymskii, P. Cloutier, and S. J. Bauer (2000), Effects of magnetic anomalies discovered at Mars on the structure of the Martian ionosphere and solar wind interaction as follows from radio occultation experiments, *J. Geophys. Res.*, *105*, 15,991, doi:10.1029/1999JA000212.

Nielsen, E., et al. (2007), Local plasma processes and enhanced electron densities in the lower ionosphere in magnetic cusp regions on Mars, *Plan. Space Sci.*, *55*(14), 2164–2172, doi:10.1016/j.pss.2007.07.003.

Picardi, G., *et al.* (2004), MARSIS: Mars Advanced Radar for Subsurface and Ionospheric Sounding, in *Mars Express: A European Mission to the Red Planet*, edited by A. Wilson, pp. 51–69 , ESA Publ. Div., Noordwijk, Netherlands.